Structures 38 (2022) 781–796

Contents lists available at ScienceDirect

Structures

journal homepage: www.elsevier.com/locate/structures

Shear response of RC beams encompassing hybrid CFRP strips and steel stirrups: Beam depth effect

Mohammad A. Alhassan [a,b,*], Rajai Z. Al-Rousan [b], Ibrahim S. Alomari [b], Layla Amaireh [a]

[a] Al-Ain University, United Arab Emirates
[b] Jordan University of Science and Technology, Jordan

ARTICLE INFO

Keywords:
Hybrid shear reinforcement
CFRP strips
Shear
RC beams
FEA

ABSTRACT

In this study, nonlinear finite element analysis (FEA) was conducted to investigate the shear behavior of reinforced concrete (RC) beams encompassing hybrid CFRP strips and steel stirrups. Primal FEA models were calibrated and verified by comparing the load–deflection response, cracking, and failure modes with the experimentally tested RC beams. A parametric case study was then implemented to evaluate the influence of critical parameters including: configurations of CFRP strips (strip width, orientation angle), size effect, and concrete compressive strength. The results showed that changing the individual CFRP strip width while maintaining a constant total width has no significant effect on the behavior of the RC beams. Increasing the concrete compressive strength improves the bond strength between the CFRP strips and concrete leading to higher load capacity. Changing the orientation angle of the CFRP strips up to 45° has minor effect on the RC beam shear capacity. The contribution of the CFRP strips was more pronounced as the beam depth increased. A comparison showed that internally-integrated CFRP strips leads to better enhancement in the shear strength of RC beams than externally strengthening with CFRP composites.

1. Introduction

Reinforced concrete (RC) is considered the most widely used construction material due to its low cost, strength, and viability to improve its characteristics through mixing with other additives [1]. The RC structures experience deteriorations as they age depending on the environmental exposure and loading, which may alter the function of the structure and the load it can resist [2]. The environmental exposure leads to corrosion of reinforcement which is the most cause of premature failure in RC structures [3]. The carbon fiber reinforced polymer (CFRP) composites have become a popular and leading technique in strengthening and repairing of RC structures due to its outstanding characteristics in terms of high strength to weight ratio, corrosion resistance, and ease of application [4–5]. The CFRP strips do not absorb moisture and thus are resistant to acid, alkali, and organic solvents. Hence, they do not undergo sizeable deterioration in saline environments where humidity is high or in the cold regions where salts are used for de-icing. Thus, CFRP strips are recognized as the most favourable material to replace the conventional steel stirrups in RC beams [6–8].

The external use of CFRP composites depends largely on the bond strength with the concrete surface, which is limited by the adhesive material properties that used to attach the CFRP composites with the concrete this limitation leads to de-bonding problems that prevent the full profitability of the CFRP composites [9–23]. Therefore, anchorage systems are used to increase the bond strength between the CFRP composites and concrete surface which leads to increase in the shear strength of RC beams [24–35]. The effectiveness of using cement-based composite systems in strengthening RC beams with FRP was compared with the epoxy-based system; it was found that the cement-based systems are more efficient than the epoxy- system in shear strengthening of RC beams [36]. Yuan and Wang [37] studied the shear behavior of concrete beams reinforced with handmade CFRP strip stirrups and CFRP longitudinal bars and found that the inclined stirrups increase the shear strength and the ductility of the beams. Evaluation of the performance of RC beams reinforced with close-type direct wound rectangular cross-section CFRP sheet strip stirrups showed that the beams that reinforced with CFRP stirrups provided better shear capacity and crack control ability compared to steel stirrups for same shear reinforcement ratio [38]. Amaireh et al. [39] found that CFRP strips can be effectively utilized as internal shear reinforcement in reinforced concrete beams, however, the use of multiple layers of CFRP strips showed lower efficiency in enhancing the shear strength than using the same strips area in

* Corresponding author.
E-mail address: mohammad.alhassan@aau.ac.ae (M.A. Alhassan).

https://doi.org/10.1016/j.istruc.2022.02.043
Received 5 August 2021; Accepted 15 February 2022
Available online 22 February 2022

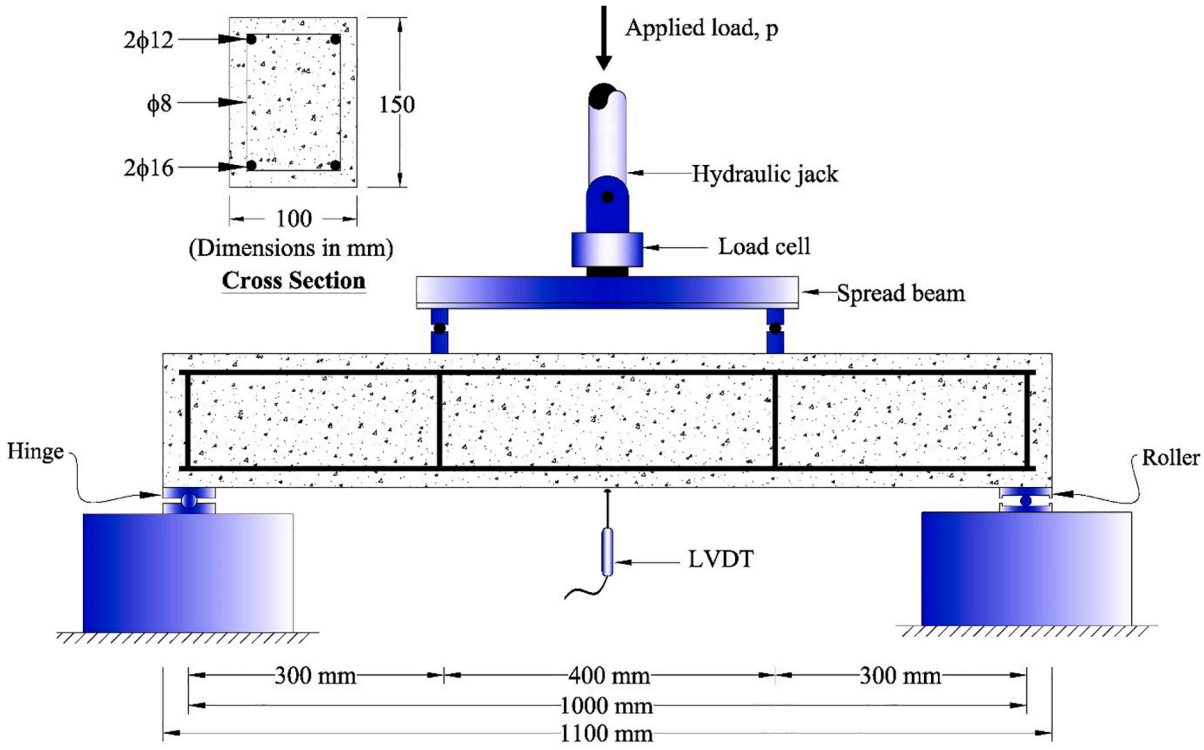

Fig. 1. Specimen dimensions, load setup and reinforcement details [39].

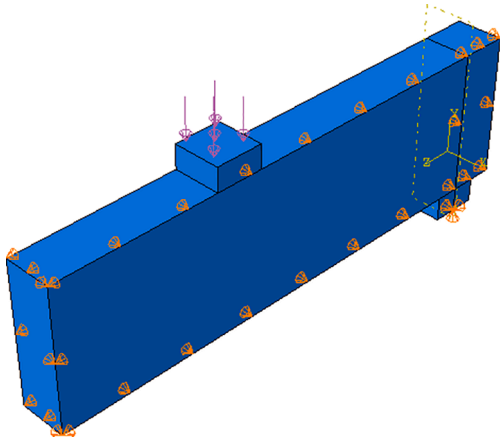

Fig. 2. Quarter model of the beam (pinned in × and in z to simulate the continuity conditions).

different locations.

The reviewed literature shows that majority of studies have looked into the benefit of using externally-attached CFRP composites to increase the strength and ductility of RC members. In general, the major parameters that affect the internal replacement of steel stirrups with CFRP strips are in the early stage of investigation, which is the direct motivation for this parametric study that followed a pioneering experimental study published recently [39]. Nonlinear FEA models were created using ABAQUS software to demonstrate the effect of critical parameters on the behavior of RC beams with internal CFRP strips including: the effect of CFRP strips width (12.5, 25 and 50 mm), the concrete compressive strength (25, 32, 40 and 60 MPa), the orientation angle of the CFRP strips (20, 30, 45°from the vertical), and the depth of the beam (150, 200, 250 mm). Proper calibration and verification of the FEA modeling was ensured based on the reputable experimental results published by Amaireh et al. [39]. The material properties, reinforcement details, and dimensions were carefully considered in the FEA modeling. In addition, a comparison between the influence of internal-integration of CFRP strips versus external attachment of CFRP composites was made.

2. Methodology

In order to verify the FEA modeling conducted in this study, eleven initial models were created and analyzed simulating the specimens tested by Amaireh et al. [39]. Eleven rectangular reinforced concrete beams were casted; one control beam without CFRP strips and ten beams received different number and configuration of CFRP strips. The beams had a cross section of 100 × 150 mm and a total length of 1100 mm. The beams were reinforced with 2ϕ16 bottom bars and 2ϕ12 top bars. Only four ϕ8 stirrups were used in each beam just to hold the bottom and top bars in place as shown in Fig. 1. The CFRP was cut in a 50 mm strips, which were attached to the beams bottom and top bars within the shear span of 300 mm from the face of the supports on both sides (one to five strips). These strips configurations were applied as one layer in a set of five beams and two layers in another set of five beams. All specimens were tested as simply supported in a four-point loading configuration as shown in Fig. 1. The simply supported span was 1000 mm and the shear span (a) was 300 mm. With an effective cross-sectional depth (d) of 125 mm, the a/d ratio is 2.4 which is intentionally selected in order to ensure that shear failure would occur in the beams within the shear span. The loading was applied using a special actuator, servo-controlled using a special data acquisition system. The mid span deflection was measured using linear variable displacement transducer (LVDT). At one beam end, two strain gages were attached to the central CFRP strip on both sides to collect the strain values. The average 28-day compressive and splitting tensile strengths were 32 MPa and 3.4 MPa, respectively. The used steel bars were Grade 60 steel with yielding strength of 420 MPa. The used carbon fiber type in this study is unidirectional in a form of tow sheet. Its thickness is 0.165 mm and produced in a 500 mm wide rolls of continuous fiber that can be cut into any appropriate lengths and width. According to the carbon fiber supplier, the carbon fiber has the

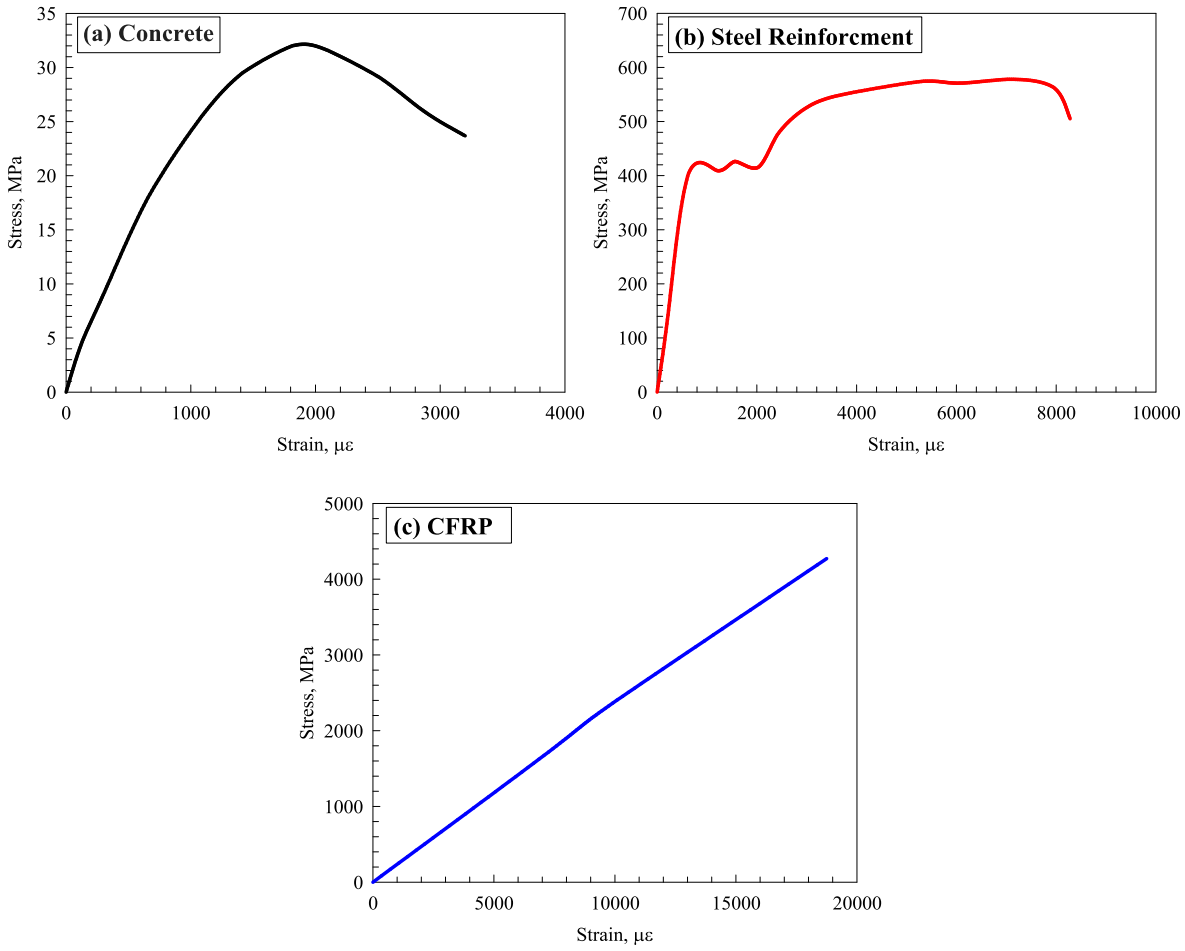

Fig. 3. Stress–strain diagrams of (a) concrete, (b) steel reinforcement, and (c) CFRP.

Table 1
Mesh sensitivity for SB1 model.

Mesh size (mm)	Number of elements	Peak load (kN)	% Error
50	33	38.5	17.559
25	264	42.5	8.994
20	672	44.7	4.283
12.5	2112	48.1	2.998

Table 2
Comparison between the FEA results and Amaireh et al. results [39].

Beam Designation	Load capacity (kN)			Ultimate deflection (mm)		
	Experimental	FEA	Error (%)	Experimental	FEA	Error (%)
Control	46.7	48.1	3.0	5.5	5.1	6.6
1S-1L	61.1	62.1	1.6	5.8	5.3	7.6
2S-1L	65.9	64.3	2.4	6.0	5.5	7.0
3S-1L	76.1	77.4	1.7	6.5	6.3	3.1
4S-1L	82.5	82.8	0.4	7.0	7.0	0.6
FS-1L	88.1	85.8	2.7	7.3	7.0	3.9
1S-2L	65.3	69.5	6.5	6.3	6.5	4.2
2S-2L	74.1	73.3	1.1	6.6	6.3	4.2
3S-2L	80.8	82.3	1.9	7.1	6.9	2.8
4S-2L	87.1	86.2	1.1	7.4	7.4	0.4
5S-2L	95.8	91.4	4.6	7.8	8.5	9.1

following characteristics: ultimate tensile strength of 4275 MPa, yielding modulus of 228 GPa, and ultimate tensile strain capacity of 0.0168 (SikaWrap®-300C). It is important to note that the CFRP strips used in this study are dry carbon fibers which are not composite materials (no epoxy is used for impregnation or curing).

2.1. Modeling and materials properties

Considering the external and continuity boundary conditions, a quarter of the beam was modelled to reduce the computational time (Fig. 2). The quarter beam had a cross section of 25 × 37.5 mm and a total length of 275 mm. The quarter beam was reinforced with 1ϕ16 bottom bars and ϕ12 top bars. Only four ϕ8 stirrups were used in each beam just to hold the bottom and top bars in place as shown in Fig. 2. This method of simulation is valid since the beams have identical experimental failure modes around their centerlines and were symmetrically loaded. The concrete is modelled using 8-node solid linear brick element (C3D8R), the steel bars were modelled using 2-node truss element (T3D2) that carries axial force only, and the CFRP strips are modelled using shell element (S4R). Fig. 3 shows the tested stress–strain diagrams for the concrete, steel reinforcement bars, and CFRP [39].

The concrete damage-plasticity model (CDPM) was used to simulate the behavior of the concrete under uniaxial and biaxial stress states [40]. The model combines damage and plasticity with failure modes that depend on tensile cracking and compression crushing. The tensile behavior can be then evaluated after calculated the main stress and strain parameters [41–46]. The concrete parameters in the CDPM were calibrated for better agreement with the experimental results. The following parameters were finally selected: dilation angle = 30°, Eccentricity 0.1, f_{b0}/f_{c0} = 1.16, K = 0.667, viscosity parameter = 0. The tensile behavior of the steel reinforcement was simulated using five segments model [47], which simulates the elastic–plastic behavior of the

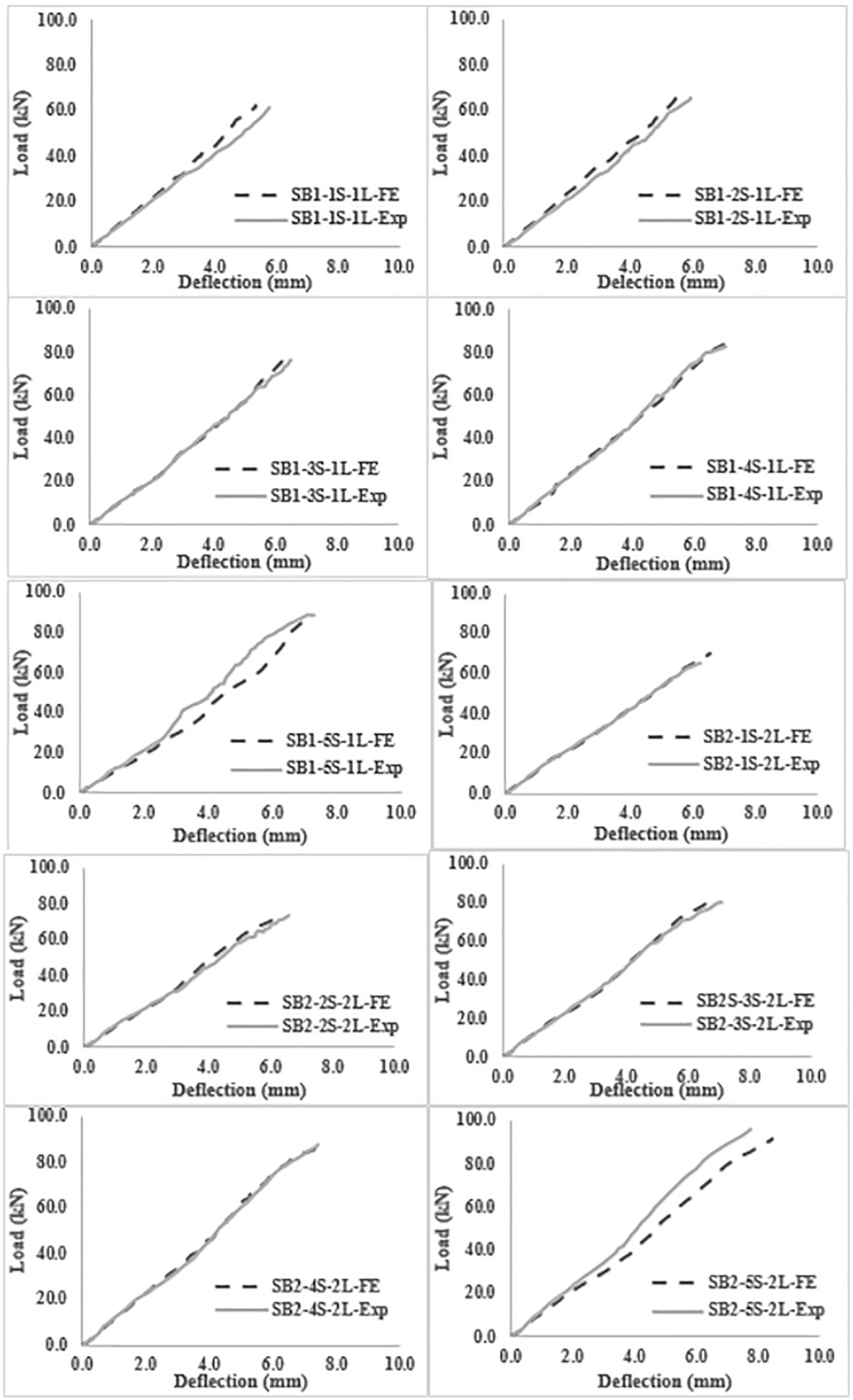

Fig. 4. Load-deflection curves for the experimental and FEA models.

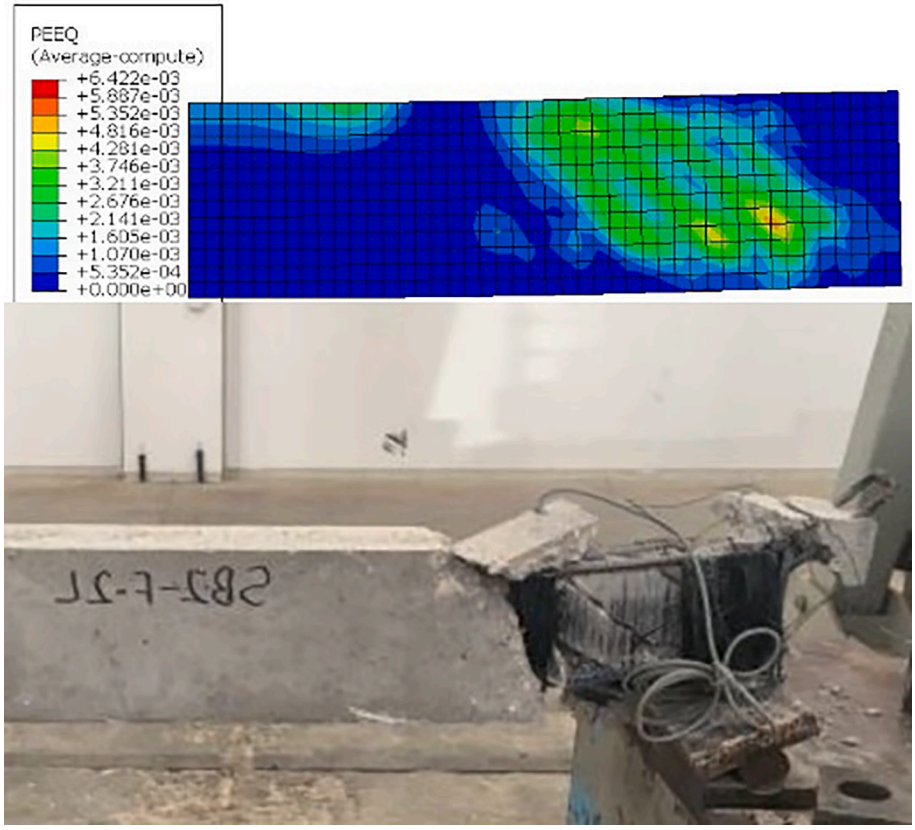

Fig. 5. Typical failure mode for the experimental specimen and FE model (SB1-FS-2L).

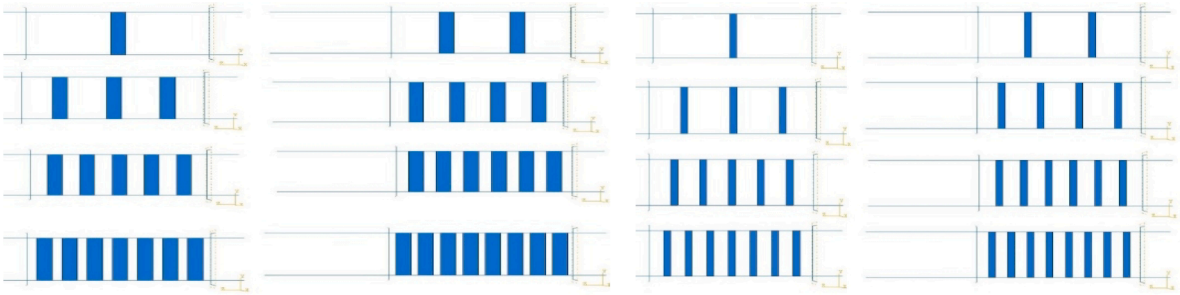

Fig. 6. Configurations of the CFRP strips with 25 mm (left) and 12.5 mm (right) widths.

steel with modulus of elasticity of steel = 200 GPa, yield stress = 420 MPa, and Poisson's ratio = 0.3.

In order to simulate the CFRP, the lamina is used to define anisotropic material where the larger stiffness and strength are in the direction of fibers. The mechanical properties of the orthotropic material are defined by the longitudinal modulus of elasticity, transverse modulus of elasticity, Poisson's ratio, and in-plane shear modulus. These parameters are determined using the rule of mixture [47] that assumes an isostrain condition (i.e. fiber and matrix have the same strain). The damage behavior of the fibers can be simulated using Hashin damage model [48], which is typically used for orthotropic material behavior. The main failure modes are fiber rupture in tension, fiber buckling in compression, matrix cracking under transverse tension and shearing, and matrix crushing under transverse compression and shearing. The damage initiation is dependent on the value of the dissipated energy, where for a given failure mode the damage is initiated if the value of the dissipated energy is equal to the critical fracture energy for that mode. The epoxy material between CFRP and concrete was simulated using the cohesion zone model (CZM), which is based on traction-separation law. This model considers tractions and separations in the normal and shear directions to the interface. The normal direction is governed by Mode-I failure, whereas the shear directions are governed by Mode-II failure. The damage evolution was modelled using energy-based linear softening using Benzeggah-Kenane (BK) fracture energy-based mode.

2.2. *Assembly and loading*

All the specimens are simply supported beams, where the loading machine and the supports are modelled by two rigid blocks with hard contact between the RC beam and the blocks. The support block is pinned in all directions on the centerline of the bottom face of the block to simulate the pin support, while the loading block is loaded on the top face to prevent the stress concentration on the loading area. Quarter of the beam is pinned in two faces, which simulates the continuity in the beam since the symmetry occurs in the loading and failure modes. The interaction between the concrete and steel reinforcement is embedded region assuming that the bond is perfect between these two materials similar to the interaction between the CFRP and concrete. This

Table 3
Designation of the FEA models used to study the effect of CFRP strip width.

Model Designation	Strip width (mm)	# of strips	# of layers
BW25-1S-1L	25	1	1
BW25-2S-1L	25	2	1
BW25-3S-1L	25	3	1
BW25-4S-1L	25	4	1
BW25-5S-1L	25	5	1
BW25-6S-1L	25	6	1
BW25-7S-1L	25	7	1
BW25-8S-1L	25	8	1
BW25-1S-2L	25	1	2
BW25-2S-2L	25	2	2
BW25-3S-2L	25	3	2
BW25-4S-2L	25	4	2
BW25-5S-2L	25	5	2
BW25-6S-2L	25	6	2
BW25-7S-2L	25	7	2
BW25-8S-2L	25	8	2
BW12.5-1S-1L	12.5	1	1
BW12.5-2S-1L	12.5	2	1
BW12.5-2S-1L	12.5	3	1
BW12.5-2S-1L	12.5	4	1
BW12.5-2S-1L	12.5	5	1
BW12.5-2S-1L	12.5	6	1
BW12.5-2S-1L	12.5	7	1
BW12.5-2S-1L	12.5	8	1
BW12.5-2S-1L	12.5	1	2
BW12.5-2S-1L	12.5	2	2
BW12.5-2S-1L	12.5	3	2
BW12.5-2S-1L	12.5	4	2
BW12.5-2S-1L	12.5	5	2
BW12.5-2S-1L	12.5	6	2
BW12.5-2S-1L	12.5	7	2
BW12.5-2S-1L	12.5	8	2

assumption was confirmed to be valid since all specimens in the experimental study [39] experienced brittle failure without slippage or bond failure. The mesh sensitivity analysis is performed to evaluate the effect of mesh size and the number of elements on the convergence of the numerical solution from the experimental results. Table 1 shows a summary of this analysis, reducing the mesh size leads to reducing the error in the peak load, while the coarse mesh size gives unrealistic damage distribution and crack pattern. Therefore, a convergence study was conducted to arrive at an optimum mesh size of 12.5 mm; the load was applied gradually to avoid sudden failure and to obtain a stable solution.

2.3. Calibration and validation

Calibration of the FEA models took into consideration the dimensions, reinforcement, and fibers details to best match the experimental results for the tested specimens by Amaireh et al. [39]. This is an essential step to ensure proper boundary conditions, mesh size, loading steps, and materials nonlinearity. To get better results and avoid sudden failure or solution divergence, the models were created with decreased loading increments. Table 2 shows the ultimate load and ultimate deflection results for the RC beams with and without CFRP strips. It is important to recall that these beams have cross-sectional dimensions of 100x150 mm with a span length 1000 mm (Fig. 1). The width of each CFRP strip is 50 mm. To explain the designation, SB1-1S-1L indicates a beam in the first group with one layer of one CFRP strip, whereas SB2-3S-2L indicates a beam in the second group with two layers of three CFRP strips. In SB1-FS-1L and SB2-FS-2L, the letter FS in the designation indicate that the CFRP was applied on the full surface of the shear span as full sheet, which is equivalent to five strips.

The results in Table 2 and Fig. 4 show excellent agreement between the FEA and experimental results with a small percent difference for all beams. The cracks pattern, deformed shapes, and failure modes were also in good agreement. Fig. 5 shows the failure mode of a beam after reaching its ultimate capacity along with the stress state near the ultimate as generated from the FEA software. It is obvious that the failed region experimentally is similar to the highly stressed region according to the FEA. The calibrated models were used to create 122 models for evaluating the effect of strips width (12.5, 25, 50 mm), concrete compressive strength (25, 32, 40, 60 MPa), orientation angle of the CFRP strips (0, 20, 30, 45°from vertical), and the depth of the beam (150, 200, 250, 300 mm).

3. Results and discussion

3.1. Effect of CFRP strips width

Three different widths of the CFRP strips were evaluated: 12.5, 25, and 50 mm (Fig. 6). Table 3 summarizes the parameters and designation of models. As shown in Fig. 7, for the models in Group I with one layer of CFRP strips (strips width = 25 mm) and for number of strips from 1 through 8, respectively, the increase in the shear capacity was approximately 8%, 30%, 37%, 47%, 56%, 64%, 70%, and 75%, in comparison with the control beam (without CFRP strips). For the FEA models in Group I with two layers of CFRP strips and for number of strips from 1 through 8, respectively, the increase in the shear capacity was approximately 15%, 39%, 49%, 60%, 67%, 74, 79, and 85%. For the FEA models in Group II with one layer of CFRP strips (strips width = 12.5 mm) and for number of strips from 1 through 8, respectively, the increase in the shear capacity was approximately 5%, 9%, 18%, 30%, 33%, 37%, 42% and 47%. For the FEA models in Group II with two layers of CFRP strips and for number of strips from 1 through 8, respectively, the increase in the shear capacity was approximately 7%, 15%, 27%, 39%, 44%, 49%, 53%, and 60%.

In order to evaluate the effect of re-arrangement of CFRP strips without changing the total width of strips, a comparison was made between the beams from Group I and Group II with the companion models that simulated the experimental results with CFRP strips width = 50 mm (Fig. 8). For one layer of strips, the increase in the shear capacity for one 50 mm strip, two 25 mm strips, and four 12.5 mm strips was almost identical and equal to 30%. Also, the increase in the shear capacity for two 50 mm strip, four 25 mm strips, and eight 12.5 mm strips was almost identical and equal to 60%. The results confirm that re-arrangement of the CFRP strips without changing the total width (regardless of the width of each individual strip) has no significant effect on the load capacity of the beams, ultimate deflection, and ductility. The gained strength is directly related to the total area of the CFRP strips. Typical stress contours in models used to evaluate the CFRP strip width effect are shown in Fig. 9.

3.2. Effect of concrete compressive strength

Three different concrete compressive strengths were studied: 25, 40, and 60 MPa, and the results were compared with the compressive strength that used in the experimental work conducted by Amaireh et al. [39], which was 32 MPa. Table 4 summarizes the parameters and designation of the FEA models.

As shown in Fig. 10, for the models in Group I with one layer of CFRP strips (compressive strength = 25 MPa) and for number of strips from 1 through 5, respectively, the increase in the shear capacity was approximately 30%, 40%, 61%, 76%, and 87%, in comparison with the control beam. For the models in Group I with two layers of CFRP strips and for number of strips from 1 through 5, respectively, the increase in the shear capacity was approximately 35%, 57%, 71%, 94% and 103%.

For Group II models with one layer of CFRP strips (compressive strength = 40 MPa) and for number of strips from 1 through 5, respectively, the increase in the shear capacity was approximately 26%, 36%, 57%, 63% and 76%. For the models in Group II with two layers of CFRP strips and for number of strips from 1 through 5, respectively, the increase in the shear capacity was approximately 35%, 53%, 67%, 76%

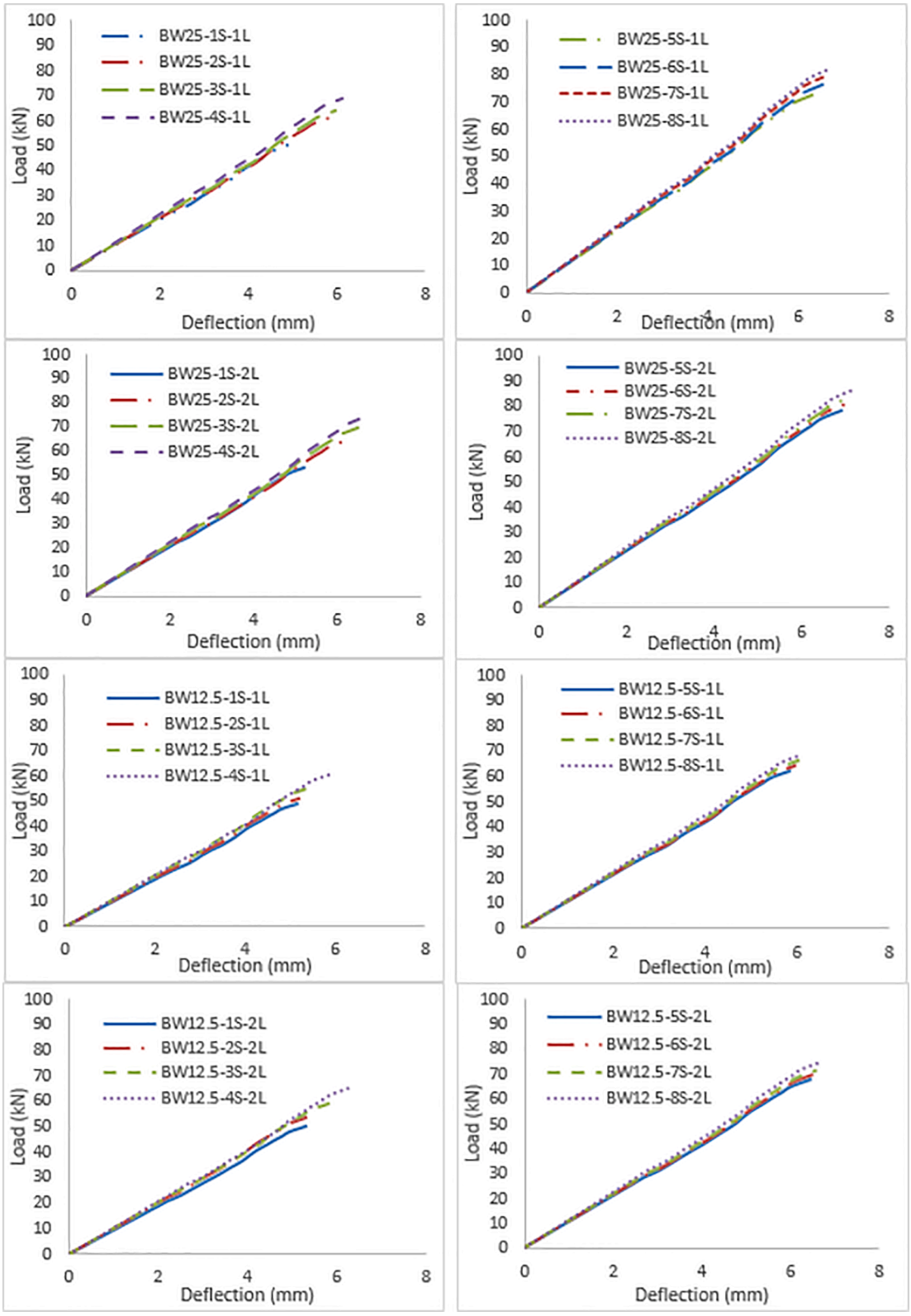

Fig. 7. Load-deflection curves for the models that illustrate the effect of CFRP strip width.

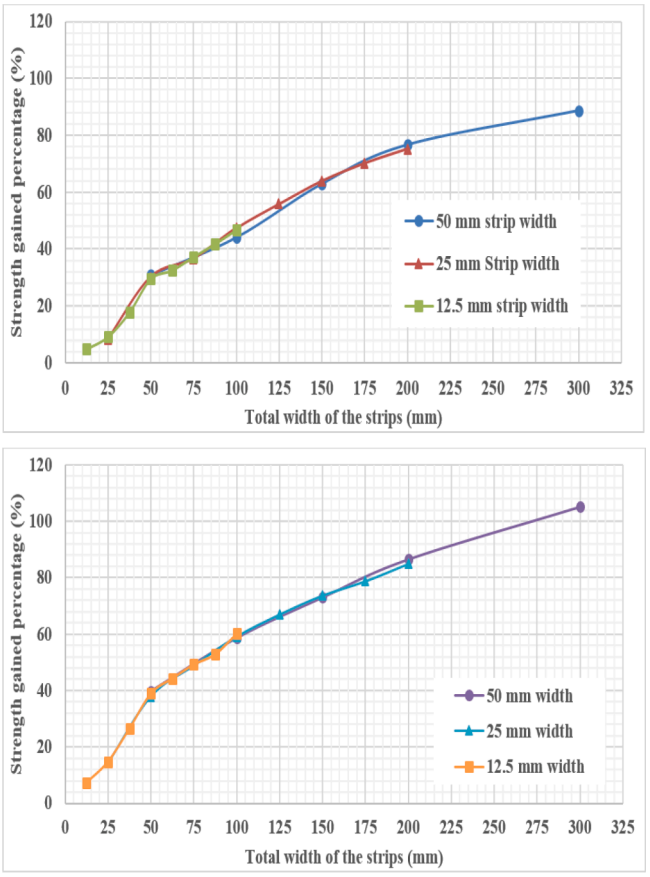

Fig. 8. Comparing different CFRP strips widths: one-layer (top) and two-layer (bottom).

and 77%. The results of four and five strips of Group II with two CFRP strips layers show that the models showed the same improvement in the shear strength; this happened due to the fact that with four CFRP strips in two layers the RC beam reached its flexural capacity as noticed in the simulation in which crushing in the compression zone occurred (the extra shear strip has no significant effect on the load capacity as the failure is transformed from shear to flexural).

For Group III models with one layer of CFRP strips (compressive strength = 60 MPa) and for number of strips from 1 through 5, respectively, the increase in the shear capacity was approximately 31%, 41%, 49%, 49% and 50%. For Group III models with two layers of CFRP strips and for number of strips from 1 through 5, respectively, the increase in the shear capacity was approximately 40%, 49%, 50%, 50% and 50%. Similar to the observation noticed above in Group II specimens, when the gain in the load capacity becomes constant, it means that the failure mode is transformed from shear into flexural.

Fig. 11 shows that the contribution of CFRP strips to the shear strength of the RC beam for various concrete compressive strength. For the models with one-strip and one layer, for concrete compressive strengths of 25, 32, 40, and 60 MPa, the CFRP strips contribution to the load capacity were 12.3., 14.4, 15.2 and 19.7 kN. This is a clear indication that as the concrete strength increases, the contribution of the

Table 4
Designation of the FEA models used to study the concrete compression strength.

Designation	Concrete compressive strength (MPa)	# of strips	# of layers
BC25	25	No CRFP strips	
BC25-1S-1L	25	1	1
BC25-2S-1L	25	2	1
BC25-3S-1L	25	3	1
BC25-4S-1L	25	4	1
BC25-5S-1L	25	5	1
BC25-1S-2L	25	1	2
BC25-2S-2L	25	2	2
BC25-3S-2L	25	3	2
BC25-4S-2L	25	4	2
BC25-5S-2L	25	5	2
BC40	40	No CFRP strips	
BC40-1S-1L	40	1	1
BC40-2S-1L	40	2	1
BC40-3S-1L	40	3	1
BC40-4S-1L	40	4	1
BC40-5S-1L	40	5	1
BC40-1S-2L	40	1	2
BC40-2S-2L	40	2	2
BC40-3S-2L	40	3	2
BC40-4S-2L	40	4	2
BC40-5S-2L	40	5	2
BC60	60	No CFRP strips	
BC60-1S-1L	60	1	1
BC60-2S-1L	60	2	1
BC60-3S-1L	60	3	1
BC60-4S-1L	60	4	1
BC60-5S-1L	60	5	1
BC60-1S-2L	60	1	2
BC60-2S-2L	60	2	2
BC60-3S-2L	60	3	2
BC60-4S-2L	60	4	2
BC60-5S-2L	60	5	2

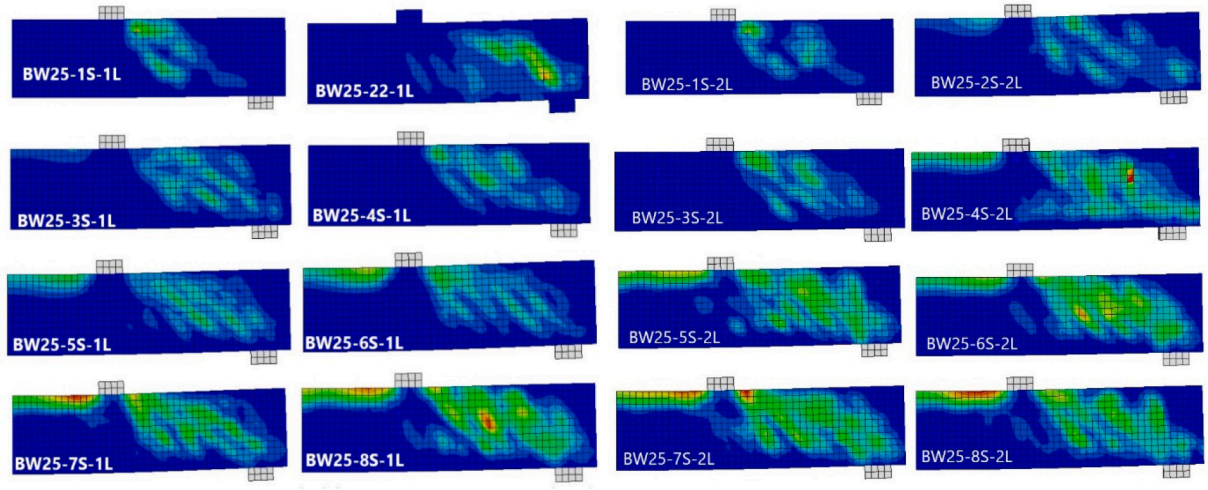

Fig. 9. Typical stress contours in models used to evaluate the CFRP strip width effect.

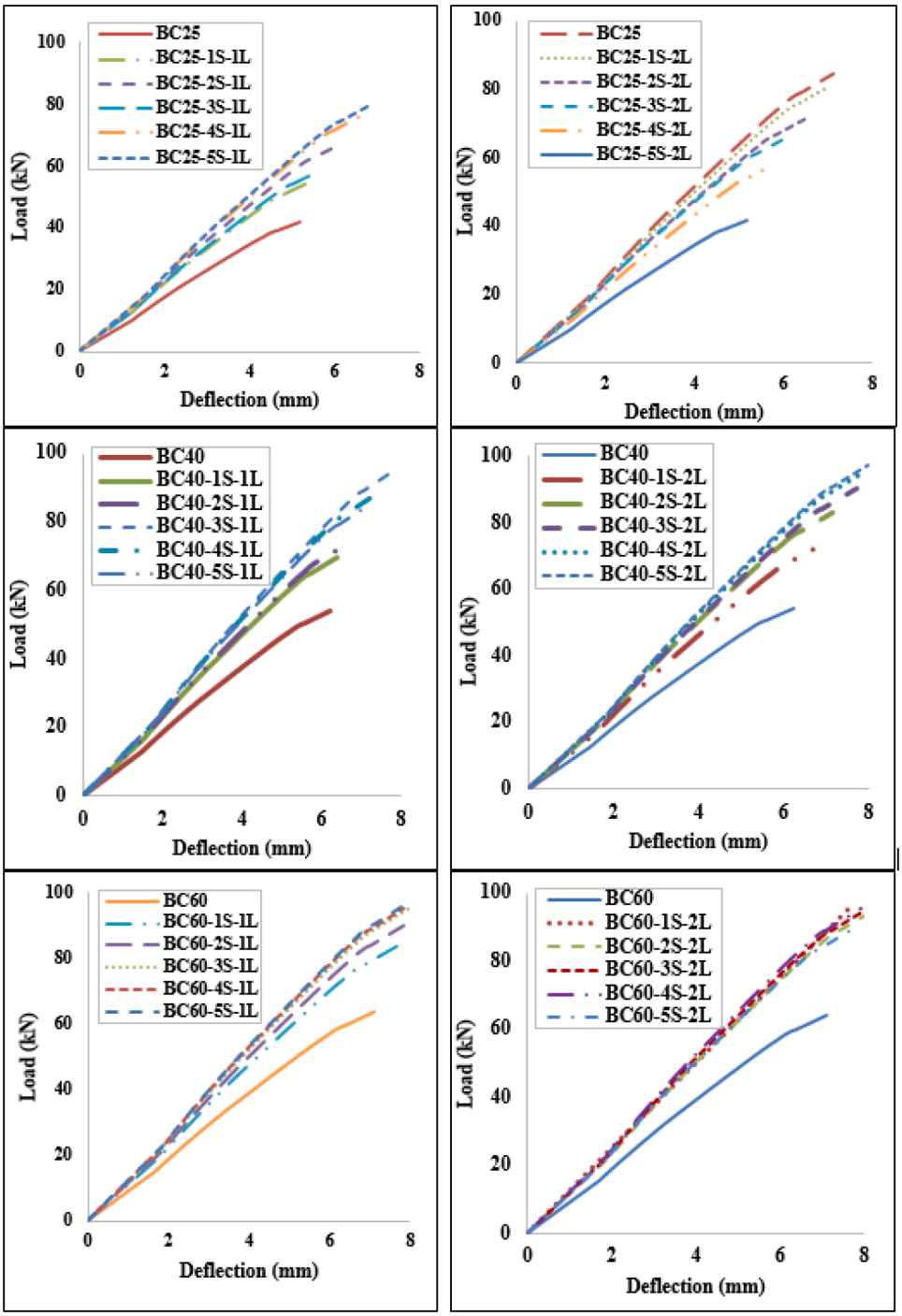

Fig. 10. Load-deflection curves for the models that illustrate effect of compressive strength.

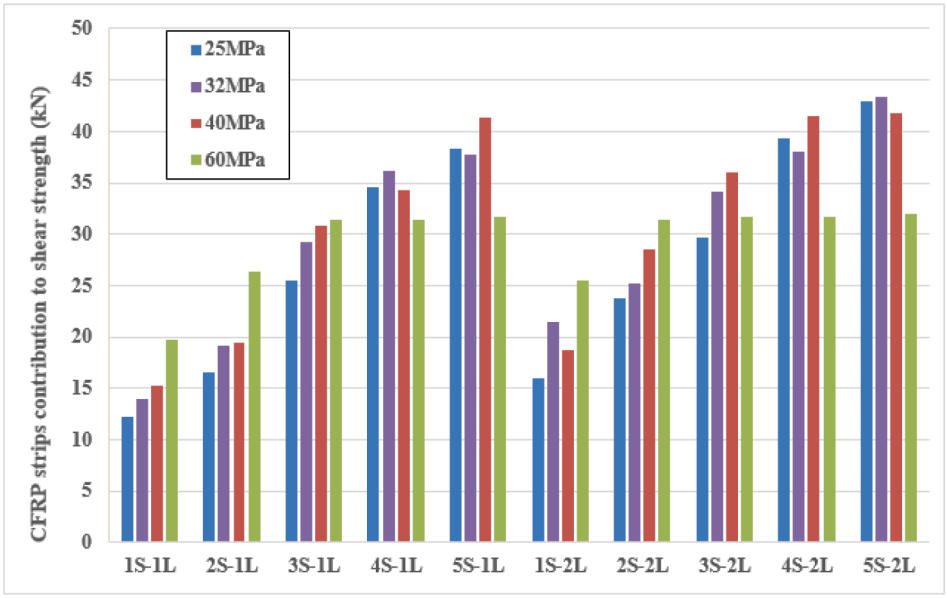

Fig. 11. CFRP strips contribution to shear strength for different concrete strength.

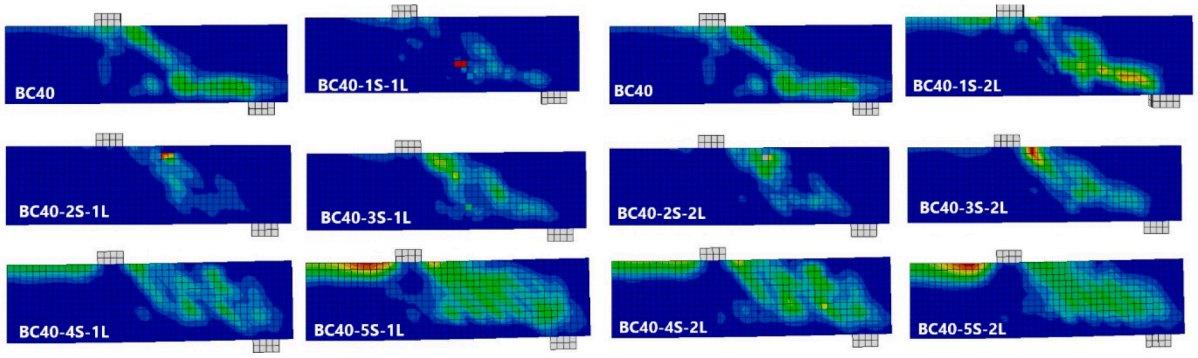

Fig. 12. Typical stress contours in models used to evaluate the compressive strength effect.

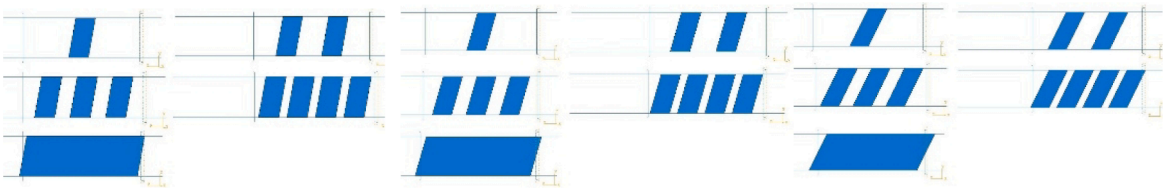

Fig. 13. Illustration of the orientation angles of the CFRP strips (20°, 30°, 45°).

Table 5
Designation of the models used to study the effect of CFRP strip orientation angle.

Designation	Orientation angle (degrees)	# of strips	# of layers
BA20-1S-1L	20	1	1
BA20-2S-1L	20	2	1
BA20-3S-1L	20	3	1
BA20-4S-1L	20	4	1
BA20-5S-1L	20	5	1
BA20-1S-2L	20	1	2
BA20-2S-2L	20	2	2
BA20-3S-2L	20	3	2
BA20-4S-2L	20	4	2
BA20-5S-2L	20	5	2
BA30-1S-1L	30	1	1
BA30-2S-1L	30	2	1
BA30-3S-1L	30	3	1
BA30-4S-1L	30	4	1
BA30-5S-1L	30	5	1
BA30-1S-2L	30	1	2
BA30-2S-2L	30	2	2
BA30-3S-2L	30	3	2
BA30-4S-2L	30	4	2
BA30-5S-2L	30	5	2
BA45-1S-1L	45	1	1
BA45-2S-1L	45	2	1
BA45-3S-1L	45	3	1
BA45-4S-1L	45	4	1
BA45-5S-1L	45	5	1
BA45-1S-2L	45	1	2
BA45-2S-2L	45	2	2
BA45-3S-2L	45	3	2
BA45-4S-2L	45	4	2
BA45-5S-2L	45	5	2

CFRP strips to the shear strength increases. This might be attributed to that as the concrete strength increases, bond between the concrete and CFRP strips increases leading to higher contribution to the shear strength. It is imperative to notice that the contribution becomes constant for companion beams with different number of CFRP strips which is attributed to that the beam flexural strength is reached. Typical stress contours in models used to evaluate the compressive strength effect are shown in Fig. 12.

3.3. Effect of orientation angle of CFRP strips

Three different orientation angles as illustrated in Fig. 13 (20, 30, and 45°from vertical) were evaluated to study the influence on the shear capacity of the RC beams. These models were used with different CFRP strips arrangement with 50 mm individual strip width, and using the same control experimental beam dimensions and reinforcement (Fig. 1). Table 5 summarizes the parameters and designation of the models.

As shown in Fig. 14, for the beams with orientation angles of 0, 20, 30, and 45° and having one layer of one strip, the shear capacities were 61.1, 62, 63.3 and 67.1 kN, respectively. These results show a slight increase in the shear capacity with increasing the orientation angle up to 45°. The achieved strength at 45° orientation angle was approximately 10% higher than the vertical configuration, while at 20° and 30° orientation angles, the increase was just 1.5% and 3.5%. For the other studied numbers of CFRP strips, similar trend can be observed as shown in Fig. 15, in which the shear strength increases slightly as the orientation angle increases up to 45°. The increase in the shear strength is expected since the inclined CFRP strips were more efficient in resisting the diagonal shear cracks.

3.4. Beam depth effect

This studied parameter is important to rationalize the observations and results of this study considering the size effect. Three different depths (200, 250, 300 mm) were evaluated having similar beam width. However, the reinforcement was changed for each bream cross-section to maintain a tension controlled failure section design. Table 6 summarizes the parameters and designation of the FEA models used to evaluate the beam depth effect. As shown in Fig. 16, for depths of 150, 200, 250 and 300 mm, the load capacities of the beams with one layer of one strip were 61.1, 83.9, 106.6 and 129.4 kN, respectively, with CFRP strip contribution to the shear strength of 14.4, 22.2, 30.5, 37.5 kN (Fig. 15). For the other studied numbers of CFRP strips, similar trend can be observed as shown in Figs. 16 and 17, in which the contribution of the CFRP strips increases as the beam depth increase for similar CFRP strips area. These results indicate that the contribution of CFRP strips to the shear strength of RC beam becomes more efficient as the beam depth increases. This can be interpreted after comparing the strains experienced by the CFRP strips at ultimate (3764, 5650, 7309 and 9760 μ) which is still lower than the ultimate tensile strain of the CFRP strips (16800 μ). In other words, the CFRP strips will contribute more to the shear strength until the full tensile capacity of the CFRP strips is reached as long as the RC beam shear capacity is not reached. Typical stress contours in the FEA models used to evaluate the beam depth effect are shown in Fig. 18.

3.5. Comparison: Internal versus external use of CFRP strips

To compare between the external and internal use of CFRP strips as shear strengthening technique, ten FEA models were created with externally-bonded CFRP strips using epoxy (composites). The ten models have the same material properties, beam dimensions, and loading setup as in the control specimens that were evaluated in the experimental study. The results shown in Table 7 indicate that the internal use of CFRP strips results in a higher contribution to the shear capacity of RC beams. This can be attributed to the full composite action that develops between the RC beam and the internal CFRP strips, whereas in the external application of CFRP strips, the composite action with the RC beam largely depends on the bonding epoxy, which typically experience failure before rupturing of the CFRP strips.

Al-Rousan [49] investigated the influence of external CFRP strips anchored with drilled grooves in the concrete surface on the shear strength of reinforced concrete beams. He used an external grooving technique in some specimens (group 2) and compared the results with companion specimens without the grooving technique (Group 1) for varied number of CFRP strips. The findings of this paper and Al-Rousan [49] paper (for similar beam depth, h = 200 mm) were compared as shown in Table 8 in terms of the percent enhancement achieved by similar area of CFRP strips with respect to control specimens. Inspection of Al-Rousan [49] results shown in Table 8 reveals that the enhancements in the beam shear strength using 50 mm external CFRP strips were 8% and 9% without and with the external grooving technique, respectively. When using 100 mm external CFRP strips, the enhancements were 14% and 17% without and with the external grooving technique, respectively. Nevertheless, the enhancements obtained using 50 mm and 100 mm of internally-integrated CFRP strips were 48% and 88%, which is a superior performance compared with the external application.

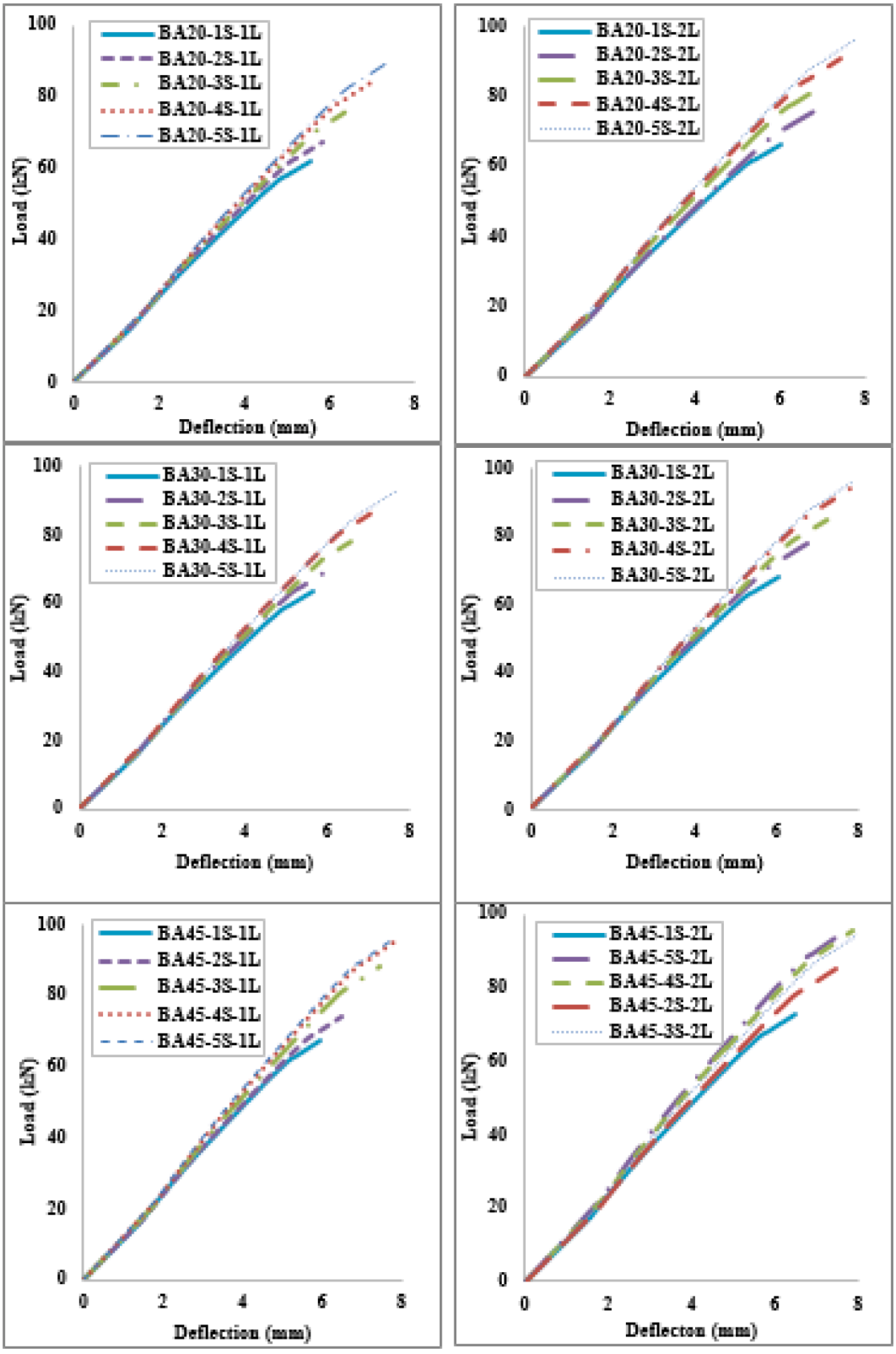

Fig. 14. Load-deflection curves for the models that illustrated the orientation angle effect.

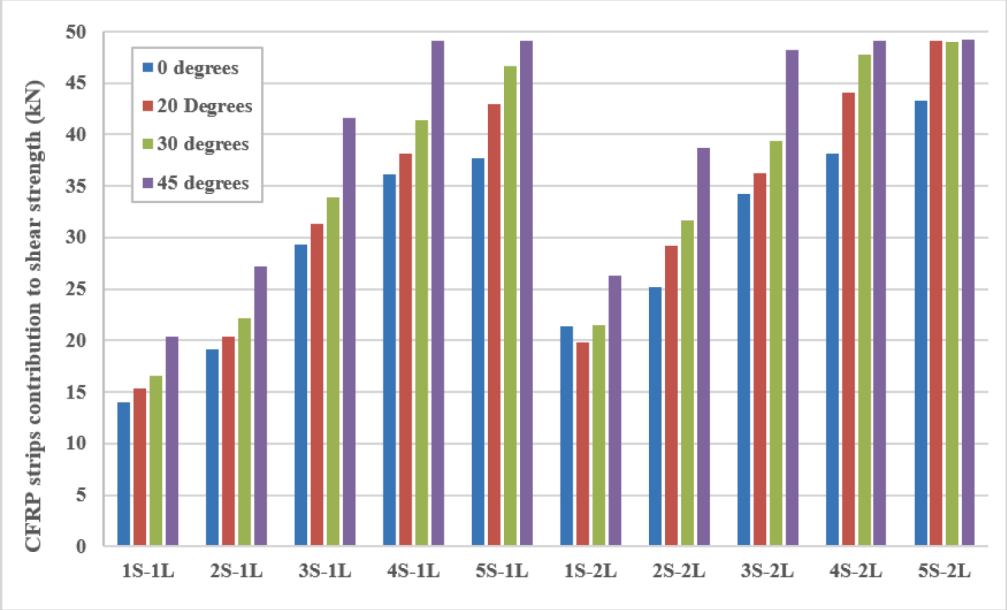

Fig. 15. CFRP shear contribution for the models with different CFRP orientation angles.

Table 6
Designation of the models used to study the effect of the beam depth.

Designation	Beam depth (mm)	# of strips	# of layers
BD20	200	No CFRP	
BD20-1S-1L	200	1	1
BD20-2S-1L	200	2	1
BD20-3S-1L	200	3	1
BD20-4S-1L	200	4	1
BD20-5S-1L	200	5	1
BD20-1S-2L	200	1	2
BD20-2S-2L	200	2	2
BD20-3S-2L	200	3	2
BD20-4S-2L	200	4	2
BD20-5S-2L	200	5	2
BD25	250	No CFRP	
BD25-1S-1L	250	1	1
BD25-2S-1L	250	2	1
BD25-3S-1L	250	3	1
BD25-4S-1L	250	4	1
BD25-5S-1L	250	5	1
BD25-1S-2L	250	1	2
BD25-2S-2L	250	2	2
BD25-3S-2L	250	3	2
BD25-4S-2L	250	4	2
BD25-5S-2L	250	5	2
BD30	300	No CFRP	
BD30-1S-1L	300	1	1
BD30-2S-1L	300	2	1
BD30-3S-1L	300	3	1
BD30-4S-1L	300	4	1
BD30-5S-1L	300	5	1
BD30-1S-2L	300	1	2
BD30-2S-2L	300	2	2
BD30-3S-2L	300	3	2
BD30-4S-2L	300	4	2
BD30-5S-2L	300	5	2

4. Conclusions

Based on the extensive nonlinear FEA conducted in this study, the following conclusions can be concluded:

1. Demonstrating a good agreement with reputable experimental results, the CDPM can be used accurately for simulating the response of RC beams with internal CFRP strips.
2. Changing the CFRP strips width while maintaining the total CFRP width constant results in comparable enhancement in the shear strength of the RC beams.
3. As the concrete compressive strength increases, the contribution of the CFRP strips to the shear strength or RC beams increases.
4. Increasing the orientation angle of the CFRP strips from 0 to 45° (from vertical) will improve the enhancement in the shear strength for similar CFRP strips area, however this improvement is minor and accordingly vertical configuration is recommended.
5. The contribution of the CFRP strips to the shear strength of RC beams is more pronounced as the beam cross-sectional depth increases.
6. For similar CFRP area, the use of CFRP strips as internal shear reinforcement improved the ultimate shear strength much better than the use of CFRP strips externally in a form of composites.
7. The findings of this study furnish a foundation for future research to tackle the behavior of deep beams with internal CFRP strips as well as to develop an analytical model for predicting the shear capacity of RC beams with internal CFRP strips.

Data Availability Statement

Some or all data, models, or code that support the findings of this study are available from the corresponding author upon reasonable request.

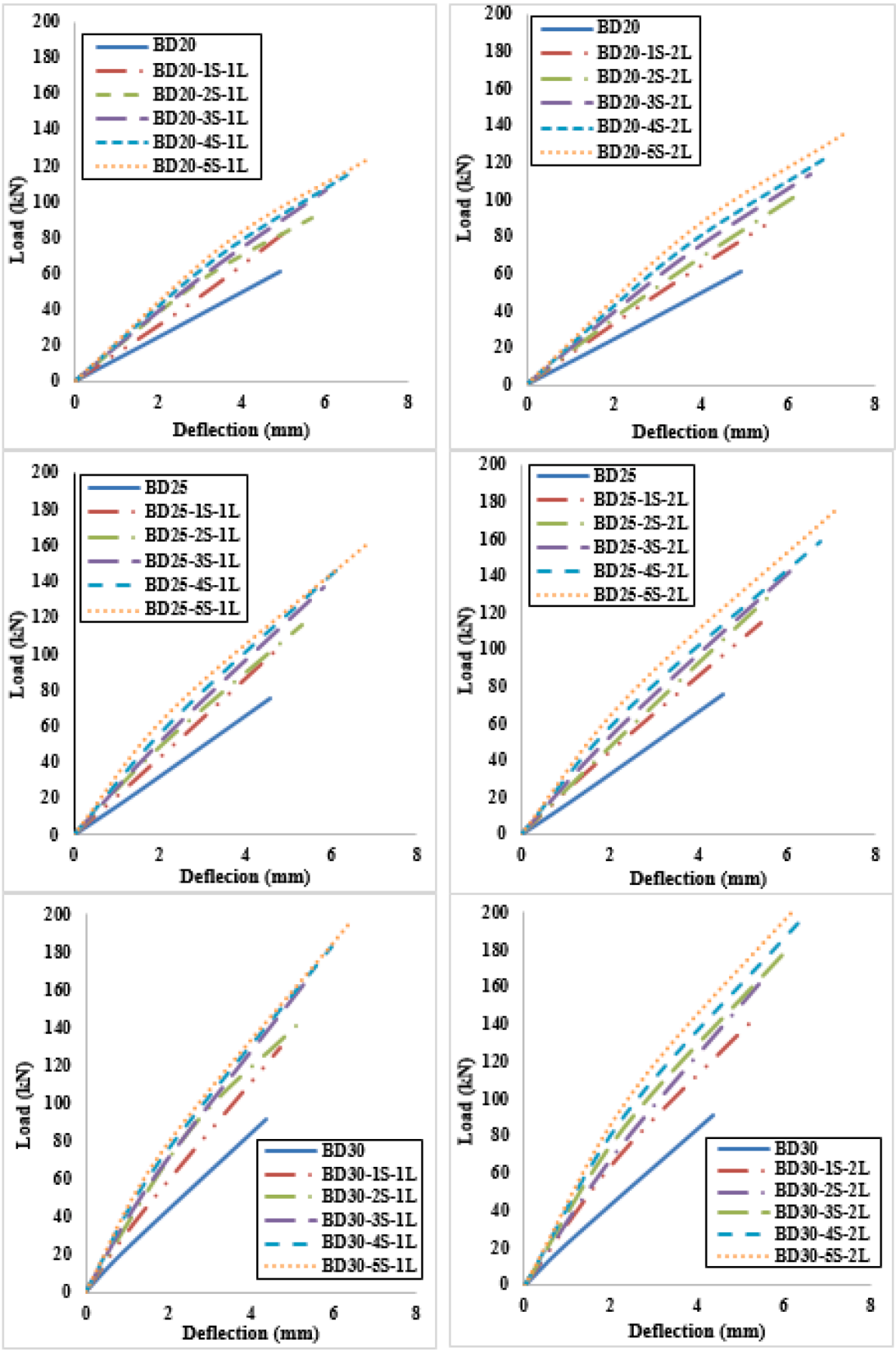

Fig. 16. Load-deflection curves for the models that illustrated the beam depth effect.

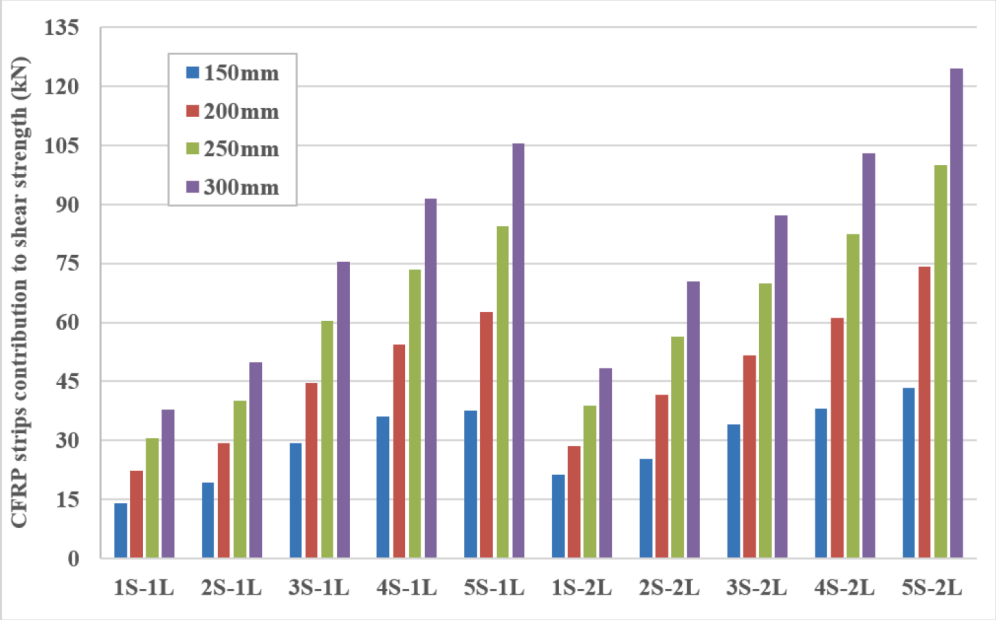

Fig. 17. Shear contribution of the CFRP strips for models with different beam depth.

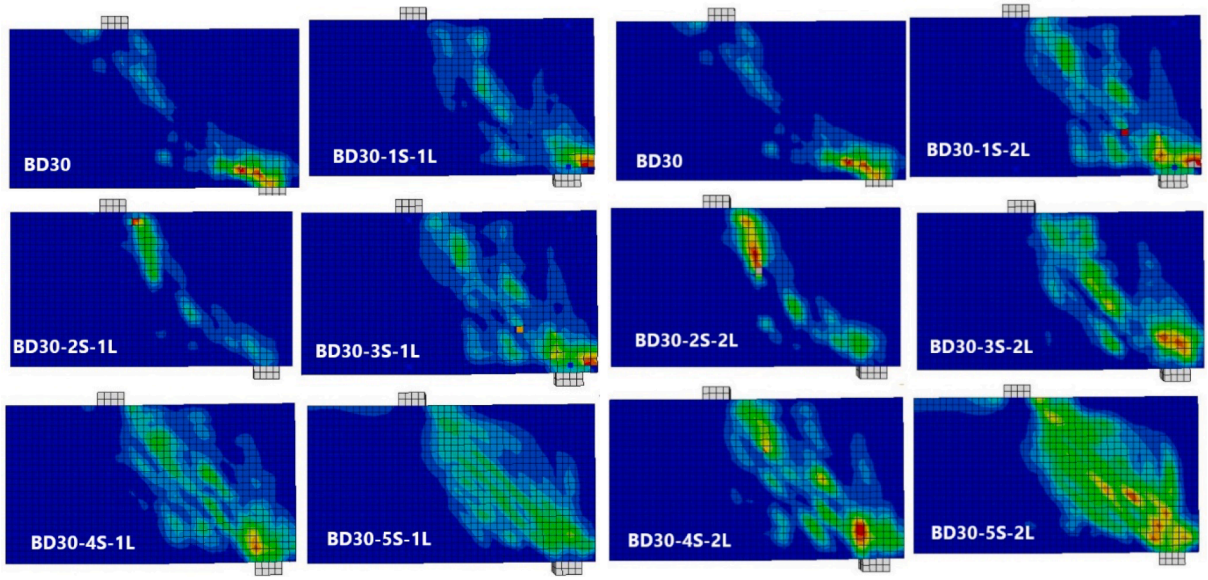

Fig. 18. Typical stress contours in models used to evaluate the beam depth effect.

Table 7
Comparison between the internal and external use of CFRP strips.

Specimen	CFRP strips contribution to the shear capacity (kN)		
	Internal use	External use	Internal/External
1S-1L	14.4	8.3	1.73
2S-1L	19.2	12.9	1.49
3S-1L	29.4	18.1	1.62
4S-1L	35.8	23.9	1.50
FS-1L	41.4	35.1	1.18
1S-2L	18.6	11.5	1.61
2S-2L	27.4	19.1	1.43
3S-2L	34.1	24.6	1.39
4S-2L	40.4	32.4	1.25
5S-2L	49.1	42.6	1.15

Table 8
Comparison with the finding of Al-Rousan [49].

CFRP strip width	Ultimate Load Capacity (kN)		
	Al-Rousan (without grooves)	Al-Rousan (with grooves)	This study
control	70.7	70.7	60
50 mm	76.2 (8%)	76.9 (9%)	89 (48%)
100 mm	80.6 (14 %)	82.6 (17%)	113 (88%)

Declaration of Competing Interest

The authors declare that they have no known competing financial interests or personal relationships that could have appeared to influence the work reported in this paper.

Acknowledgment

The authors gratefully acknowledge the continuous support from the Jordan University of Science and Technology and Al Ain University.

References

[1] ACI Code 318-14, Building code requirements for structural concrete and commentary, an ACI Standard, American Concrete Institute, Farmington Hills, MI, 2014.
[2] Alhassan MA, Al RZ, Rousan EA, Shuqari Al. Bond-slip behavior between fiber reinforced concrete and CFRP composites. Ain Shams Eng J 2019;10(12):359–67.
[3] Ormellese M, Berra M, Bolzoni F, Pastore T. Corrosion inhibitors for chlorides induced corrosion in reinforced concrete structures. Cem Concr Res 2006;36(3):536–47.
[4] Kadhim MMA, Adheem AH, Jawdhari AR. Nonlinear Finite Element Modelling and Parametric Analysis of Shear Strengthening RC T-Beams with NSM CFRP Technique. Int J Civ Eng. 2019;17(8):1295–306.
[5] Hawileh RA, Abdalla JA, Naser MZ. Modeling the shear strength of concrete beams reinforced with CFRP bars under unsymmetrical loading. Mech Adv Mater Struct 2019;26(15):1290–7.
[6] Almusallam TH, Al-Salloum YA. Durability of GFRP Rebars in Concrete Beams under Sustained Loads at Severe Environments. J Compos Mater 2006;40(7):623–37.
[7] Porter ML, Barnes BA. Accelerated aging degradation of glass fiber composites. Second Int Conf Compos Infrast 1998;2:446–59.
[8] Ellyin F, Rohrbacher C. Effect of Aqueous Environment and Temperature on Glass-Fibre Epoxy Resin Composites. J Reinf Plast Compos 2000;19(17):1405–27.
[9] Chaallal O, Nollet M-J, Perraton D. Shear Strengthening of RC Beams by Externally Bonded Side CFRP Strips. J Compos Constr 1998;2(2):111–3.
[10] Triantafillou T. Shear Strengthening of Reinforced Concrete Beams Using Epoxy-Bonded FRP Composites. ACI Struct J 1998;95.
[11] Khalifa A, Nanni A. Improving shear capacity of existing RC T-section beams using CFRP composites. Cem Concr Compos 2000;22(3):165–74.
[12] Li G, Zhang A, Jin W. Effect of Shear Resistance on Flexural Debonding Load-Carrying Capacity of RC Beams Strengthened with Externally Bonded FRP Composites. Polymers. 2014;6(5):1366–80.
[13] Chen JF, Teng JG. Shear capacity of FRP-strengthened RC beams: FRP debonding. Constr Build Mater 2003;17(1):27–41.
[14] Zhang Z, Hsu C-T. Shear Strengthening of Reinforced Concrete Beams Using Carbon-Fiber-Reinforced Polymer Laminates. J Compos Constr 2005;9(2):158–69.
[15] Mosallam AS, Banerjee S. Shear enhancement of reinforced concrete beams strengthened with FRP composite laminates. Compos B Eng 2007;38(5-6):781–93.
[16] Bousselham A, Chaallal O. Mechanisms of Shear Resistance of Concrete Beams Strengthened in Shear with Externally Bonded FRP. J Compos Constr 2008;12(5):499–512.
[17] Pannirselvam N, Nagaradjane V, Chandramouli K. Strength Behaviour of Fibre Reinforced Polymer Strengthened Beam. Journal of Engineering and Applied Sciences. 2009;4:34–9.
[18] El-Sayed AK. Effect of longitudinal CFRP strengthening on the shear resistance of reinforced concrete beams. Compos B Eng 2014;58:422–9.
[19] Mabrouk AG, Osman MR. Finite Element Modeling Of RC Beams Shear-Strengthened With Side Bonded CFRP Sheets. The 6th Asia Pacific Conference on FRP in Structures. 2017;1:19-25.
[20] Saadoon AS. Effect of CFRP Strips Orientation on Performance of Strengthened Deep Beams. Al-Qadisiyah J Eng Sci 2019;12:172–7.
[21] Thamrin R, Zaidir, Haris S, Awaludin A, Matsumoto T, Pessiki S, et al. Shear capacity of reinforced concrete beams strengthened with web side bonded CFRP sheets. MATEC Web of Conf 2019;258:04010. https://doi.org/10.1051/matecconf/201925804010.
[22] Mhanna HH, Hawileh RA, Abdalla JA. Shear Strengthening of Reinforced Concrete Beams Using CFRP Wraps. Proc Struct Integrity 2019;17:214–21.
[23] Oller E, Pujol M, Marí A. Contribution of externally bonded FRP shear reinforcement to the shear strength of RC beams. Compos B Eng 2019;164:235–48.
[24] Galal K, Mofidi A. Shear Strengthening of RC T-Beams Using Mechanically Anchored Unbonded Dry Carbon Fiber Sheets. J Perform Constr Facil 2010;24(1):31–9.
[25] Chaallal O, Mofidi A, Benmokrane B, Neale K. Embedded Through-Section FRP Rod Method for Shear Strengthening of RC Beams: Performance and Comparison with Existing Techniques. J Compos Constr 2011;15(3):374–83.
[26] Mofidi A, Chaallal O, Benmokrane B, Neale K. Performance of End-Anchorage Systems for RC Beams Strengthened in Shear with Epoxy-Bonded FRP. J Compos Constr 2012;16(3):322–31.
[27] Kim Y, Quinn K, Ghannoum WM, Jirsa JO. Shear Strengthening of Reinforced Concrete T-Beams Using Anchored CFRP Materials. ACI Struct J 2014;111:1027–36.
[28] Shomali A, Mostofinejad D, Esfahani MR. Shear strengthening of RC beams using EBRIG CFRP strips: a comparative study. European Journal of Environmental and Civil Engineering. 2021;25(14):2540–56.
[29] Zhou Y, Guo M, Sui L, Xing F, Hu B, Huang Z, et al. Shear strength components of adjustable hybrid bonded CFRP shear-strengthened RC beams. Compos B Eng 2019;163:36–51.
[30] Hadhood A, Agamy MH, Abdelsalam MM, Mohamed HM, Aly El-Sayed T. Shear strengthening of hybrid externally-bonded mechanically-fastened concrete beams using short CFRP strips: Experiments and theoretical evaluation. Eng Struct 2019;201:109795. https://doi.org/10.1016/j.engstruct.2019.109795.
[31] Kalupahana WKKG, Ibell TJ, Darby AP. Bond characteristics of near surface mounted CFRP bars. Constr Build Mater 2013;43:58–68.
[32] Alhassan MA, Al-Rousan RZ, Taha HM. Precise finite element modelling of the bond-slip contact behavior between CFRP composites and concrete. Constr Build Mater 2020;240:117943. https://doi.org/10.1016/j.conbuildmat.2019.117943.
[33] Al-Rousan RZ. Empirical and NLFEA prediction of bond-slip behavior between DSSF concrete and anchored CFRP composites. Constr Build Mater 2018;169(1):530–42.
[34] Al-Rousan RZ and AL-Tahat MF. Consequence of surface preparation techniques on the bond behavior between concrete and CFRP composites. Construction and Building Materials, 2019; 212:62-374.
[35] Iovinella I, Prota A, Mazzotti C. Influence of surface roughness on the bond of FRP laminates to concrete. Constr Build Mater 2013;40:533–42. https://doi.org/10.1016/j.conbuildmat.2012.09.112.
[36] Azam R, Soudki K, West JS, Noël M. Strengthening of shear-critical RC beams: Alternatives to externally bonded CFRP sheets. Constr Build Mater 2017;151:494–503.
[37] Yuan Ye, Wang Z. Shear behavior of large-scale concrete beams reinforced with CFRP bars and handmade strip stirrups. Compos Struct 2019;227:111253. https://doi.org/10.1016/j.compstruct.2019.111253.
[38] Tahir M, Wang Z, Ali KM, Isleem HF. Shear behavior of concrete beams reinforced with CFRP sheet strip stirrups using wet-layup technique. Structures. 2019;22:43–52.
[39] Amaireh L, Al-Rousan RZ, Ababneh AN, Alhassan M. Integration of CFRP strips as an internal shear reinforcement in reinforced concrete beams. Structures. 2020;23:13–9.
[40] Lee J, Fenves GL. Plastic-Damage Model for Cyclic Loading of Concrete Structures. J Eng Mech 1998;124(8):892–900.
[41] Lubliner J, Oliver J, Oller S, Onate E. Plastic-damage model for concrete. Int J Struct 1989;26:252.
[42] Alfarah B, López-Almansa F, Oller S. New methodology for calculating damage variables evolution in Plastic Damage Model for RC structures. Eng Struct 2017;132:70–86.
[43] Wahalathantri BL, Thambiratnam DP, Chan THT, Fawzia S. A Material Model For Flexural Crack Simulation In Reinforced Concrete Elements Using Abaqus. Infrastructure: Transport and Urban Development; 2008. p. 260–4.
[44] Yusuf S, Aktaş M. Defining parameters for concrete damage plasticity model. Challenge J Struct Mech 2015;1:149–55.
[45] M. Nikbin I, Rahimi R. S, Allahyari H. A new empirical formula for prediction of fracture energy of concrete based on the artificial neural network. Eng Fract Mech 2017;186:466–82.
[46] V.Chaudhari S, A. Chakrabarti M. Modeling of Concrete for Nonlinear Analysis using Finite Element Code ABAQUS. Int J Comput Appl 2012;44(7):14–8.
[47] Birtel V, Mark B. Parameterised Finite Element Modelling of RC Beam Shear Failure. Inst Reinforced Prestressed Concr Struct Abstract 2006;1:95–108.
[48] Hashin Z. Fatigue Failure Criteria for Unidirectional Fiber Composites. J Appl Mech 1981;48:846–52.
[49] Al-Rousan RZ. Impact of elevated temperature and anchored grooves on the shear behavior of reinforced concrete beams strengthened with CFRP composites. Case Stud Constr Mater 2021;14:e00487. https://doi.org/10.1016/j.cscm.2021.e00487.